

A machine learning approach to identify structural connections affected in diffuse axonal injury

J. Mitra¹, S. Ghose¹, K-K. Shen¹, K. Pannek², P. Bourgeat¹, J. Frapp¹, O. Salvado¹, J. L. Mathias³, D. J. Taylor⁴, and S. Rose¹

¹Australian e-Health & Research Centre, CSIRO Digital Productivity Flagship, Herston, QLD, Australia, ²Imperial College London, London, United Kingdom, ³School of Psychology, University of Adelaide, Adelaide, SA, Australia, ⁴Dept. of Radiology, The Royal Adelaide Hospital, Adelaide, SA, Australia

Introduction: Studies suggest that approximately 20% of patients admitted to hospital due to traumatic brain injury (TBI) have sustained moderate or severe head injuries, with the other 80% having mild injuries. Many patients with mild TBI sustain diffuse axonal injury (DAI)¹ which is microscopic in nature and difficult to detect using conventional MRI. Diffusion MRI, along with probabilistic tractography, is ideally suited to detect DAI within specific white matter (WM) pathways. These approaches, based on measures of structural connectivity, can be used to identify damaged neural pathways in group-wise analyses of TBI and healthy control cohorts². In contrast to standard statistical connectomic analysis (*t*-test), recent interest has focussed on more advanced machine learning methods to discriminate between the diseased and healthy groups⁴.

We present a new method to identify significantly different and discriminative structural connections between the TBI and healthy control groups by integrating a statistical GLM-based (generalized linear model) network clustering and random forest classifier.

Method: Our study examined 180 TBI patients and 145 age-matched normal controls with no head injury. The MRI data were acquired using a 3T Siemens TimTrio (Siemens, Erlangen, Germany) scanner. A high angular resolution diffusion imaging (HARDI) echo-planar imaging (EPI) sequence in 64 directions with $b=3000\text{s/mm}^2$ were acquired. A field map was acquired using two 2D gradient recalled echo images (TE1/TE2 4.76/7.22 ms) to assist the correction for distortion due to susceptibility inhomogeneities. An extensive preprocessing procedure was used to detect and correct for image artefacts caused by involuntary head motion, cardiac pulsation, and image distortions for the diffusion-weighted images⁵. The T1-weighted 1 mm isotropic images were segmented for the brain tissues⁶ (gray-matter (GM), white-matter (WM) & cerebrospinal fluid (CSF)) and the subcortical GM structures were segmented by registering⁷ to an AAL (anatomical atlas labelling) atlas of 116 regions (including cortical and subcortical regions). Finally, the PVE maps for GM and WM were generated⁸ for seeding the tractography algorithm. Anatomically constrained tractography (ACT)⁹ was performed using MRtrix¹⁰. The streamlines were further filtered (SIFT)¹¹ to reduce bias due to the seeding strategy.

Mean FA values along the streamlines connecting each pair of AAL regions were encoded in a 116×116 network connectivity matrix. The connectivity matrices were then contrasted for a group-wise comparison between the TBI and the healthy groups using network based statistics¹² (NBS). Two different *t*-thresholds of 3.0 and 3.5 with 5000 permutations and $p < 0.05$ were chosen for NBS group-wise comparison. The lower threshold returned 116 connections, while the higher threshold returned 24 connections, which were significantly different between the groups.

The FA values of the respective connections obtained from NBS were then used as features for a random forest (RF) classifier¹³. The feature dimension was reduced (retaining 95% energy) using principal component analysis (PCA) for 116 connections (NBS, $t=3.0$) and the features were only projected to the co-variance space using PCA for 24 connections (NBS, $t=3.5$). The RF classifier consisted of 50 fully-grown trees with the default *sqrt*(feature dimension) parameter for random sampling. The parameters were chosen after extensive experimentation on the number of trees, tree depth and the number of variables to sample in order to prevent over-fitting. The classification performance was validated using a 10-fold cross-validation (1/10th of the dataset was left out during training and the classification was tested on this set) repeated over 100 times. The feature relevancies of the best discriminating features were obtained from the RF *gini* importance. The features in the projected principal component (PC) space, were mapped back to the network connectivity domain by tracing the maximum absolute weight of a feature connection in the respective PC ('B4' method)¹⁴.

Results: The RF classification on the significant connections obtained from NBS (*t*-threshold=3.0, Fig. 1(a)) revealed an average sensitivity of $82.19\% \pm 1.87\%$ in identifying TBI patients from normal controls with an overall accuracy of $70.45\% \pm 1.59\%$. While RF classification after NBS (*t*-threshold=3.5, Fig. 1(b)) could not sufficiently discriminate TBI from normal controls (Table 1). RF classification further provided a list of 28 discriminative structural connections from the set of 116 (NBS, $t=3.0$, $p < 0.05$) statistically significant connections. Some of the discriminative and statistically significant connections are shown in Fig. 2.

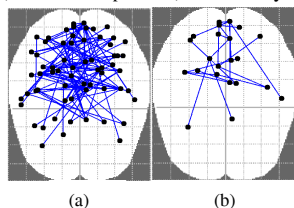


Fig. 1 Significant network differences with NBS between TBI and healthy control groups. (a) NBS with $t=3.0$, (b) NBS with $t=3.5$.

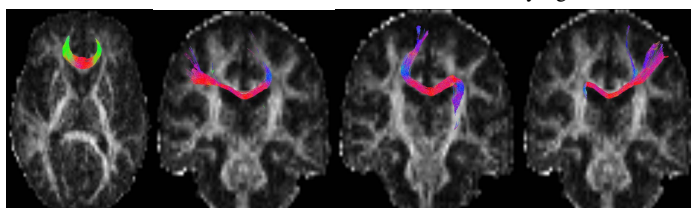


Fig. 2 Discriminative and statistically significant connections from RF (left to right): 1) Superior_Frontal_Gyrus_Medial_R – Gyrus_Rectus_L, 2)Supplementary_Motor_Area_R – Postcentral_Gyrus_R, 3) Paracentral_Lobule_L – Thalamus_R, 4) Precentral_Gyrus_R – Caudate_Nucleus_L.

Table 1 Quantitative evaluation of the proposed method (NBS + RF) to discriminate between TBI and healthy controls. Sensitivity (<i>Sens.</i>), Specificity (<i>Spec.</i>), Accuracy (<i>Acc.</i>)			
<i>Method</i>	<i>Sens.</i> (%)	<i>Spec.</i> (%)	<i>Acc.</i> (%)
NBS($t=3.0$) + RF	82.19 ± 1.87	55.86 ± 2.44	67.30 ± 1.84
NBS($t=3.5$) + RF	72.55 ± 1.99	60.78 ± 2.84	70.45 ± 1.59

Discussion: This study (NBS, $t=3.0$ & RF) revealed that structural connections along the corpus callosum, superior frontal gyrus, subcortical GM structures and cingulum are most affected by DAI in TBI patients. Even though statistical methods like *t*-tests have the capability of identifying statistically significant connections that differ between the two groups, these structural connections may not be discriminative. While boosting- and bagging- based random forest classifier in addition to GLM-based methods appears to provide more discriminative connections. Our proposed method employing NBS for feature selection, while employing RF classification, provides a means of refining the features; thus exploiting the benefits of both statistical and machine learning methods for detecting altered WM connectivity.

References: 1. Meythaler, J.M. et al. Current concepts: diffuse axonal injury-associated traumatic brain injury. *Arch. Phys. Med. Rehabil.* 2001; 82:1461-1471. 2. Arfanakis, K. et al. Diffusion tensor MR imaging in diffuse axonal injury. *Am. J. Neuroradiol.* 2002; 23:794-802. 3. Achard, S. et al. Hubs of brain functional networks are radically reorganized in comatose patients. *Proc. Natl. Acad. Sci. U.S.A.* 2012; 109:20608-20613. 4. Deshpande, G. et al. Identification of neural connectivity signatures of autism using machine learning. *Frontiers in Human Neuroscience.* 2013; 7:1-15. 5. Pannek, K. et al. Diffusion MRI of the neonate brain: acquisition, processing and analysis technique. *Pediatr Radiol.* 2012; 42:1169-1182. 6. van Leemput, K. et al. Automated model-based tissue classification of MR images of the brain. *IEEE Trans. in Med. Imag.* 1999; 18:897-908. 7. Modat, M. et al. Fast free-form deformation using graphics processing units. *Comp. Meth. & Prog. in Biomed.* 2010; 98:278-284. 8. Acosta, O. et al. Automated voxel-based 3D cortical thickness measurement in a combined Lagrangian-Eulerian PDE approach using partial volume maps. *Med. Image Anal.* 2009; 13:730-743. 9. Smith, R. et al. Anatomically-constrained tractography: improved diffusion MRI streamlines tractography through effective use of anatomical information. *NeuroImage.* 2012; 63:1924-1938. 10. Tournier, J.D. et al. MRtrix: Diffusion tractography in crossing fiber regions. *Intl. J. of Imag. Sys. & Tech.* 2012; 22:53-66. 11. Smith, R. et al. SIFT: spherical-deconvolution informed filtering of tractograms. *NeuroImage.* 2013; 67:298-312. 12. Zalesky, A. et al. Network-based statistic: Identifying differences in brain networks. *NeuroImage.* 2010; 53:1197-1207. 13. Breiman, L. Random forests. *Machine Learning.* 2001; 45. 14. Jolliffe, I.T. Principal Component Analysis. Second ed., Springer-Verlag, 2002; New York.